



# Influence of calcium and magnesium on the secondary structure in solutions of individual caseins and binary casein mixtures



Manpreet Kaur Grewal <sup>a</sup>, Todor Vasiljevic <sup>a</sup>, Thom Huppertz <sup>a, b, c, \*</sup>

<sup>a</sup> Advanced Food Systems Research Unit, Institute for Sustainable Industries and Liveable Cities, Victoria University, Melbourne, VIC 8001, Australia

<sup>b</sup> FrieslandCampina, Amersfoort, the Netherlands

<sup>c</sup> Wageningen University and Research, Wageningen, the Netherlands

## ARTICLE INFO

### Article history:

Received 14 January 2019

Received in revised form

2 September 2020

Accepted 11 September 2020

Available online 28 September 2020

## ABSTRACT

The influence of Ca and Mg addition on the secondary structure of  $\alpha_{S1}$ -,  $\alpha_{S2}$ -,  $\beta$ - and  $\kappa$ -CN in solutions of individual and binary mixtures of caseins was investigated using FTIR spectroscopy. Both in individual and their binary mixtures, addition of Ca and Mg resulted in increase in  $\beta$ -sheet structures and decrease in triple helices and turns, implying binding of cations to similar sites. Binding of cations with phosphoserine clusters with loop-helix-loop motifs explained the reduction in helical element. In addition, the binding of cations to electronegative regions reduced electrostatic repulsion, resulting in an increase in hydrophobic interactions accounting for increase in sheet structures. Compared with Mg, it seemed that Ca had more affinity for caseins, especially when they were in a binary mixture. The information presented here expands the present understanding of casein interactions.

© 2020 The Authors. Published by Elsevier Ltd. This is an open access article under the CC BY license (<http://creativecommons.org/licenses/by/4.0/>).

## 1. Introduction

Casein micelles are colloidal complexes of four types of caseins ( $\alpha_{S1}$ -,  $\alpha_{S2}$ -,  $\beta$ - and  $\kappa$ -CN) held together by amorphous calcium phosphate, electrostatic and hydrophobic forces (Huppertz, Fox, & Kelly, 2018). Casein micelles carry approximately two thirds of the total milk calcium, half the inorganic phosphate, one third of magnesium, and smaller proportions of citrate and the other small ions (Bijl, Huppertz, van Valenberg, & Holt, 2018). Thus, the casein micelles are perceived as a biological transport vehicle for calcium, phosphorous and protein for neonates (Holt, Carver, Ecroyd, & Thorn, 2013). However, some differences exist in distribution of calcium in the micelle and its interaction with different caseins. This is mainly due to a lack of information as caseins could not be crystallised and hence complete secondary and tertiary structure is not available. For the same reason, NMR and X-ray crystallography, otherwise effective tools for studying in detail the interactions of the protein with itself and with other ions and molecules in solution, has not proven of much use in the case of caseins (Sawyer et al., 2002). Nonetheless, spectroscopic techniques (Raman, Fourier transform infrared spectroscopy, Circular dichroism) and

molecular modelling have given some interesting insights on secondary structure of caseins and their interactions with calcium, sodium and potassium (Curley, Kumosinski, Unruh, & Farrell, 1998; Farrell, Brown, & Malin, 2013; Huppertz, 2013).

Calcium-casein interactions appear to occur primarily via serine phosphate groups as demonstrated by <sup>31</sup>P nuclear magnetic resonance (NMR) (Kakalis, Kumosinski, & Farrell, 1990). However, Fourier transform infrared (FTIR) spectroscopy revealed that calcium also binds to negatively charged carboxylate groups of glutamate and aspartate residues in a freeze-dried casein (Byler & Farrell, 1989). In addition, FTIR spectroscopy has demonstrated potential to show subtle changes in the secondary structural elements that are associated with changes in protein environment in aqueous solutions. On addition of Ca<sup>2+</sup> to caseinate solutions containing K<sup>+</sup> and Na<sup>+</sup>, binding of Ca<sup>2+</sup> to casein resulted in redistribution of the components of its FTIR spectra. An apparent decrease in large loop or helical structures at 37 °C was observed, concomitant with increase in the percentage of structures having greater bond energy, such as turns and extended helical structures (Curley et al., 1998). As serine phosphate side chains are known to have a loop-helix-loop conformation, the changes in loops and helical structures with addition of Ca<sup>2+</sup> further supported the idea that these are the sites for Ca<sup>2+</sup> binding in caseins. Furthermore, the swelling of the casein structure observed upon incorporation of Ca<sup>2+</sup> into reformed micelles at 37 °C could be reinforced by a shift in

\* Corresponding author. Tel.: +31 6 11187512.

E-mail address: [Thom.Huppertz@frieslandcampina.com](mailto:Thom.Huppertz@frieslandcampina.com) (T. Huppertz).

absorbance to higher wave numbers (greater bond energies) (Curley et al., 1998). However, most work has been carried either on whole casein or single protein systems, and also in the absence of either Ca or Mg. FTIR analysis of changes in conformation when casein is present in solution with another casein (binary mixtures) and in absence and presence of two known cations of casein micelle  $\text{Ca}^{2+}$  and  $\text{Mg}^{2+}$  would thus expand present understanding of casein micelles.

Hence in this study, the secondary structure of individual caseins ( $\alpha_{\text{S1-}}$ ,  $\alpha_{\text{S2-}}$ ,  $\beta$ - and  $\kappa$ -CN) and the changes incurred when present with another casein in the similar ratio as in milk, in the absence or presence of  $\text{Ca}^{2+}$  or  $\text{Mg}^{2+}$ , were investigated using FTIR spectroscopy.

## 2. Material and methods

### 2.1. Materials

Four caseins  $\alpha_{\text{S1-}}$ ,  $\alpha_{\text{S2-}}$ ,  $\beta$ - and  $\kappa$ -CN were obtained from stocks present at NIZO (Ede, The Netherlands).  $\kappa$ -CN was prepared as described by Leaver and Law (1992),  $\alpha_{\text{S2-}}$ -CN as described by Snoeren, Van Der Spek, & Payens (1977) and  $\alpha_{\text{S1-}}$ -casein as described by Mulvihill and Fox (1977);  $\beta$ -casein was purchased from Eural (Nantes, France). All casein preparations contained >95% protein on dry matter and >95% of the target casein out of total protein, as determined by RP-HPLC (Visser, Slangen, & Rollema, 1991). Casein stock solutions (20 mg mL<sup>-1</sup>) were prepared in 25 mM PIPES buffer containing 100 mM KCl. Binary mixtures of caseins (with total casein concentration 20 mg mL<sup>-1</sup>) were prepared at a ratio of 1:1 ( $\alpha_{\text{S1-}}$ -CN +  $\beta$ -CN;  $\alpha_{\text{S2-}}$ -CN +  $\kappa$ -CN) or 4:1 ( $\alpha_{\text{S1-}}$ -CN +  $\alpha_{\text{S2-}}$ -CN;  $\alpha_{\text{S1-}}$ -CN +  $\kappa$ -CN;  $\beta$ -CN +  $\alpha_{\text{S2-}}$ -CN;  $\beta$ -CN +  $\kappa$ -CN) from these stock solutions. Stock solutions and binary mixtures were subsequently mixed with 25 mM PIPES +100 mM KCl or 25 mM PIPES +70 mM KCl +10 mM  $\text{CaCl}_2$  or 25 mM PIPES +70 mM KCl +10 mM  $\text{MgCl}_2$  to attain a final casein concentration of 10 mg mL<sup>-1</sup> and a Ca or Mg concentration of 0, 2.5, 5 or 10 mmol L<sup>-1</sup>.

### 2.2. FTIR measurements and spectral data analysis

FTIR spectra were acquired in the range of 4000 to 600 cm<sup>-1</sup> at 25 °C using a PerkinElmer Frontier FTIR spectrometer (PerkinElmer, Boston, MA, USA) with a resolution of 4 cm<sup>-1</sup> and averaging 16 scans for each spectrum. Approximately 0.5 mL of sample was added onto an attenuated total reflectance (ATR; PerkinElmer Universal ATR Accessory, single reflection) cell. A background spectrum was scanned at the beginning of the measurements with a blank Diamond ATR cell using same instrumental conditions as for the sample spectra acquisition. FTIR experiments for individual caseins, binary mixture without Ca and Mg were replicated twice (on two sets of samples) whereas binary mixture with different concentrations of Ca/Mg did not have replicates. Each sample spectra was analyzed twice using curve fitting procedure.

The FTIR spectra of all samples were exported to Unscrambler Version 10.2 software (CAMO AS, Trondheim, Norway). Spectra were baseline-corrected and then the spectrum of the respective buffer was subtracted as described previously (Grewal et al., 2017). Subsequently, the spectra were subjected to standard normal variate (SNV) pretreatment. The SNV-treated spectra were then exported to Origin software (Origin Pro 2017, Origin Lab Corp, Northampton, MA, USA) to perform non-linear curve fitting procedure as described elsewhere (Grewal, Huppertz, & Vasiljevic, 2018) to quantify the changes in the secondary structure of individual caseins with modifications in their environment.

Briefly, the buffer-subtracted SNV transformed spectra of amide I region was baseline corrected and deconvoluted (FSD 15, 0.18).

The deconvoluted spectra were further smoothed (3-point moving average) and the peaks were identified using second derivative and fitted with a Gaussian function using the Peak fit procedure in an Origin software. The program iterated the curve-fitting process, and in each iteration, the characteristic parameters (height, bandwidth, position and baseline) were varied to calculate the parameters that would result in the best fit of the deconvoluted protein spectrum using Gaussian shaped curves. Optimal fits to spectra were indicated by reduced chi-square values and it was ensured visually that fit did not include assigned peaks below the baseline or with too broad or too narrow bandwidths. The peak fit observed in this study had low chi-square ( $1 \times 10^{-6}$ ) and residual ( $\pm 0.05$ ) values, indicating a good fit (Grewal et al., 2018). Once a good fit was obtained, the band area for each component peak assigned to specific secondary structure was used to calculate the relative contribution of component to a particular secondary structure. Five features depicting main protein secondary structures, namely  $\alpha$ -helix (1654–1658 cm<sup>-1</sup>),  $\beta$ -sheet (1623–1643 and 1689–1698 cm<sup>-1</sup>),  $\beta$ -turns (1666–1687 cm<sup>-1</sup>), random coils (1646–1650 cm<sup>-1</sup>) and  $3_{10}$ -helix (1660–1666 cm<sup>-1</sup>), were assigned to different peaks in the second derivative spectra. Significance of changes in the secondary structure was further evaluated at 95% confidence level using one-way ANOVA followed by Tukey's HSD multi-comparison test (IBM SPSS Statistics 25).

Principal component analysis (PCA) was also employed for data in the protein amide I region spanning from 1700 to 1600 cm<sup>-1</sup> to better understand the changes in the conformation of caseins induced by different environments, i.e., individual or mixture or different cation in the buffer quantified using curve fitting procedure. PCA score plots demonstrate groupings of samples, whereas the loading plots aided in identifying wavenumbers which have high loadings or contributed the most in classification of samples into different groups. In addition, as the wavenumbers could be assigned to particular secondary structures, PCA could identify specific changes in the secondary structure of caseins in response to a particular environment.

## 3. Results and discussion

### 3.1. Secondary structure of individual caseins

In this study, FTIR spectra of caseins and mixtures thereof were determined at a total protein content of 10 mg mL<sup>-1</sup>. This casein concentration was selected because it approximates the concentrations of  $\alpha_{\text{S1-}}$  and  $\beta$ -casein in bovine milk. Furthermore, this concentration is also sufficiently high to avoid notable contributions of protein adsorption on the ATR cell, which Goldberg and Chaffotte (2005) reported was particularly strong at protein concentrations < 3 mg mL<sup>-1</sup>.

Individual caseins, when suspended in PIPES buffer containing only K<sup>+</sup> as cation, indicated a significant amount of secondary structure, as also reported in previous studies (Byler, Farrell, & Susi, 1988; Farrell, Brown, Hoagland, & Malin, 2003; Holt & Sawyer, 1993; Huppertz, 2013). Quantitative analysis revealed that  $\alpha_{\text{S1-}}$ -CN had the most ordered structure, with 38%  $\beta$ -sheet, 15%  $\alpha$ -helical structure and 16%  $3_{10}$ -helix followed by  $\alpha_{\text{S2-}}$ -CN with 35%  $\beta$ -sheet, 14%  $\alpha$ -helix and 15%  $3_{10}$ -helix (Table 1). Proportions of  $\alpha$ -helix and  $\beta$ -sheet in  $\alpha_{\text{S1-}}$ -CN estimated in this study agree with previous reports by Malin, Brown, Wickham, & Farrell (2005) who reported 13–15%  $\alpha$ -helix and 34–46% extended  $\beta$ -sheet-like structures in that protein. The main features of the  $\alpha_{\text{S2-}}$ -CN casein structure are in agreement with the findings of Hoagland, Unruh, Wickham, & Farrell (2001), who suggested 24–32%  $\alpha$ -helix, 27–37%  $\beta$ -sheet, 24–31% turns and 9–22% unspecified structure. Significantly higher helical structure in both of these caseins compared with  $\beta$ -

**Table 1**  
Quantification of secondary structure of individual caseins and their respective binary mixtures using a curve fitting of amide I.<sup>a</sup>

Casein	Area (%)				
	$\alpha$ -helices	Total $\beta$ -sheet	Random	$3_{10}$ -helix	$\beta$ -turns
$\alpha_{S1}$ -CN	14.8 <sup>a</sup>	38.2 <sup>a</sup>	14.5 <sup>a</sup>	15.6 <sup>a</sup>	12.5 <sup>a</sup>
$\alpha_{S2}$ -CN	14.2 <sup>a</sup>	34.9 <sup>b</sup>	12.2 <sup>b</sup>	14.9 <sup>ab</sup>	20.5 <sup>b</sup>
$\beta$ -CN	11.0 <sup>b</sup>	29.7 <sup>c</sup>	14.7 <sup>a</sup>	14.3 <sup>b</sup>	18.0 <sup>c</sup>
$\kappa$ -CN	12.6 <sup>c</sup>	32.6 <sup>d</sup>	10.7 <sup>c</sup>	10.8 <sup>c</sup>	21.8 <sup>d</sup>
$\alpha_{S1}$ -CN + $\alpha_{S2}$ -CN (4:1)	10.3 <sup>bd</sup>	39.6 <sup>f</sup>	10.5 <sup>c</sup>	12.5 <sup>d</sup>	20.2 <sup>b</sup>
$\alpha_{S1}$ -CN + $\beta$ -CN (1:1)	14.8 <sup>a</sup>	36.9 <sup>a</sup>	11.3 <sup>de</sup>	11.2 <sup>ce</sup>	18.9 <sup>c</sup>
$\alpha_{S1}$ -CN + $\kappa$ -CN (4:1)	12.8 <sup>c</sup>	34.1 <sup>be</sup>	11.8 <sup>be</sup>	12.0 <sup>de</sup>	20.4 <sup>b</sup>
$\beta$ -CN + $\alpha_{S2}$ -CN (4:1)	9.8 <sup>d</sup>	33.2 <sup>de</sup>	10.6 <sup>cd</sup>	11.3 <sup>ce</sup>	20.4 <sup>b</sup>
$\alpha_{S2}$ -CN + $\kappa$ -CN (1:1)	9.6 <sup>d</sup>	40.2 <sup>f</sup>	10.6 <sup>cd</sup>	11.8 <sup>cde</sup>	21.2 <sup>bd</sup>
$\beta$ -CN + $\kappa$ -CN (4:1)	9.9 <sup>d</sup>	40.1 <sup>f</sup>	11.0 <sup>cd</sup>	12.0 <sup>de</sup>	20.4 <sup>b</sup>

<sup>a</sup> Binary mixtures were prepared at a ratio indicated in parentheses. Values are means (n = 2); means in the same column that do not share the same small letters differ significantly (P < 0.05). Wavenumbers are:  $\alpha$ -helices, 1651–1653 cm<sup>-1</sup>; total  $\beta$ -sheet, 1619–1642 and 1688–1697 cm<sup>-1</sup>; random, 1644–1648 cm<sup>-1</sup>;  $3_{10}$ -helix, 1661–1664 cm<sup>-1</sup>;  $\beta$ -turns, 1667–1678 cm<sup>-1</sup>.

CN and  $\kappa$ -CN could be attributed to loop-helix-loop motif centred on their phosphoserine clusters. Highest  $\beta$ -sheet percentages in  $\alpha_{S1}$ -CN and  $\alpha_{S2}$ -CN are also consistent with their pH and ionic strength-dependent self-association characteristics at the given ionic strength of 0.1 used in this study. Both these caseins being amphipathic self-associate primarily via hydrophobic domains (involving sheet and turn structures) and to some extent via H-bonding as the dissociation does not occur at low temperatures. Comparatively lower  $\beta$ -sheet in  $\alpha_{S2}$ -CN compared with  $\alpha_{S1}$ -CN can be explained by lower hydrophobicity, three anionic clusters, intra and inter molecular disulphide bonding, and 40% lower prolyl residues in the former, and hence less extensive self-association (Huppertz, 2013; Swaisgood, 2003).

$\beta$ -CN is the casein with the lowest level of ordered (30%  $\beta$ -sheet, 11%  $\alpha$ -helix) and maximum random structures (15%) (Table 1). The secondary structure of  $\beta$ -CN was in a range as reported by previous studies (Creamer, Richardson, & Parry, 1981; Farrell, Wickham, Unruh, Qi, & Hoagland, 2001; Qi, Wickham, & Farrell, 2004; Qi,

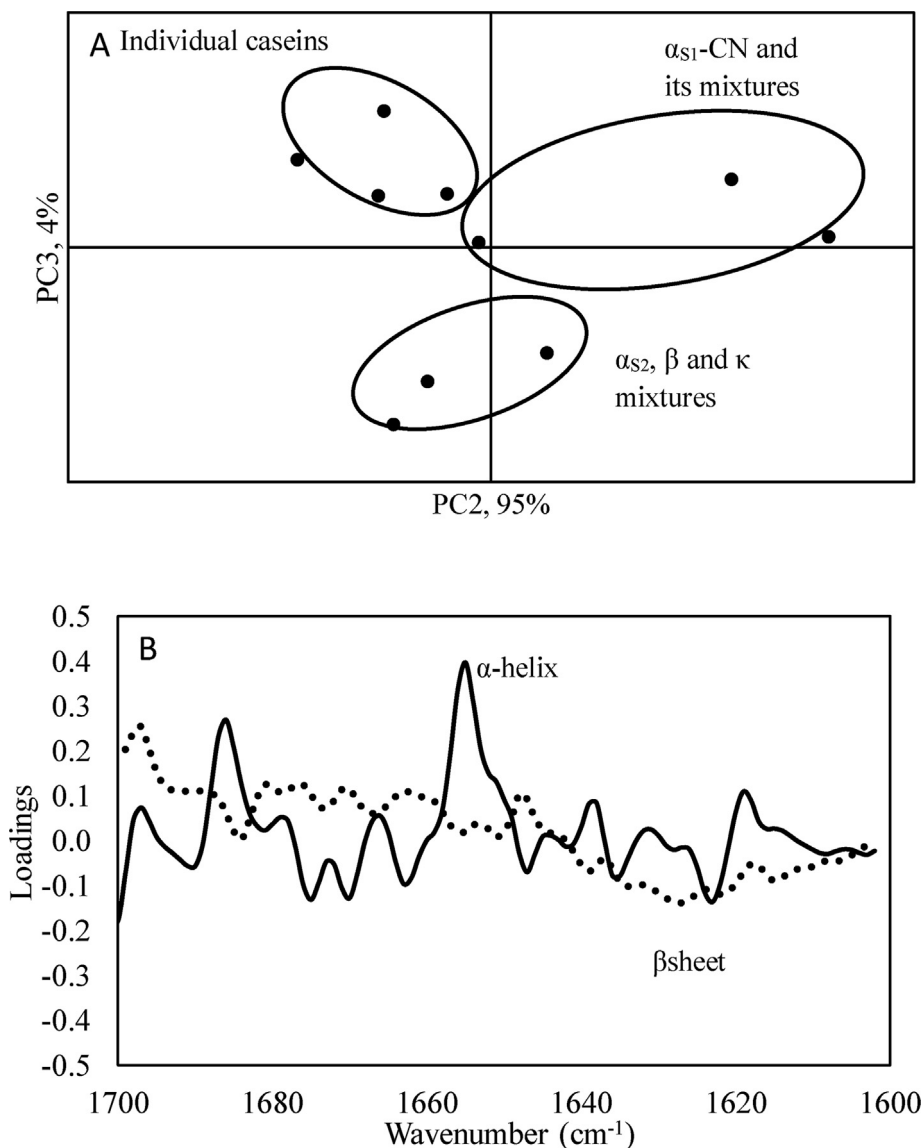


**Fig. 1.** PCA plot (A) with loadings (B; ..... , PC2; —, PC3) of FTIR data in the region 1700–1600 cm<sup>-1</sup> for individual caseins and their binary mixtures in PIPES buffer containing 100 mM KCl (buffer 1).

**Table 2**Total percentage areas of different secondary structures in amide I for  $\alpha_{S1}$ -casein,  $\alpha_{S2}$ -casein,  $\beta$ -casein and  $\kappa$ -casein in PIPES buffer without or with Ca or Mg.<sup>a</sup>

Added Ca or Mg (mM)	$\alpha$ -helix	Total $\beta$ -sheet	Random	$3_{10}$ -helix	Total $\beta$ -turns
$\alpha_{S1}$ -casein					
0	14.8 <sup>a</sup>	38.2 <sup>a</sup>	14.5 <sup>a</sup>	15.6 <sup>a</sup>	12.5 <sup>a</sup>
2.5 Ca	12.0 <sup>b</sup>	43.8 <sup>b</sup>	11.2 <sup>bf</sup>	8.7 <sup>b</sup>	16.8 <sup>c</sup>
5.0 Ca	12.6 <sup>bd</sup>	43.0 <sup>c</sup>	11.6 <sup>b</sup>	10.3 <sup>c</sup>	13.6 <sup>b</sup>
10.0 Ca	11.7 <sup>b</sup>	43.2 <sup>c</sup>	12.2 <sup>c</sup>	7.1 <sup>d</sup>	13.8 <sup>b</sup>
2.5 Mg	20.8 <sup>c</sup>	44.7 <sup>e</sup>	9.0 <sup>d</sup>	—	18.0 <sup>d</sup>
5.0 Mg	13.3 <sup>d</sup>	38.0 <sup>a</sup>	10.3 <sup>e</sup>	8.2 <sup>e</sup>	22.1 <sup>e</sup>
10.0 Mg	11.9 <sup>b</sup>	41.0 <sup>d</sup>	10.6 <sup>ef</sup>	8.5 <sup>f</sup>	20.5 <sup>f</sup>
$\alpha_{S2}$ -casein					
0	14.2 <sup>a</sup>	34.9 <sup>a</sup>	12.2 <sup>a</sup>	14.9 <sup>a</sup>	20.5 <sup>a</sup>
2.5 Ca	10.8 <sup>be</sup>	45.9 <sup>b</sup>	10.3 <sup>b</sup>	7.9 <sup>b</sup>	17.2 <sup>b</sup>
5.0 Ca	10.6 <sup>bce</sup>	45.0 <sup>c</sup>	8.3 <sup>c</sup>	10.7 <sup>c</sup>	13.4 <sup>c</sup>
10.0 Ca	10.4 <sup>bc</sup>	44.1 <sup>d</sup>	10.7 <sup>d</sup>	8.4 <sup>d</sup>	16.0 <sup>d</sup>
2.5 Mg	10.0 <sup>c</sup>	39.0 <sup>c</sup>	10.9 <sup>d</sup>	8.9 <sup>e</sup>	21.8 <sup>e</sup>
5.0 Mg	13.3 <sup>d</sup>	39.0 <sup>e</sup>	10.0 <sup>e</sup>	7.9 <sup>b</sup>	20.5 <sup>a</sup>
10.0 Mg	11.1 <sup>e</sup>	40.5 <sup>f</sup>	11.8 <sup>a</sup>	8.6 <sup>d</sup>	18.6 <sup>f</sup>
$\beta$ -casein					
0	11.0 <sup>a</sup>	29.7 <sup>a</sup>	14.7 <sup>a</sup>	14.3 <sup>a</sup>	18.3 <sup>a</sup>
2.5 Ca	10.7 <sup>a</sup>	37.6 <sup>b</sup>	11.4 <sup>b</sup>	7.7 <sup>b</sup>	20.2 <sup>b</sup>
5.0 Ca	10.0 <sup>b</sup>	34.7 <sup>c</sup>	14.3 <sup>ac</sup>	9.0 <sup>c</sup>	16.1 <sup>c</sup>
10.0 Ca	9.9 <sup>b</sup>	37.4 <sup>b</sup>	15.2 <sup>a</sup>	8.4 <sup>d</sup>	14.2 <sup>d</sup>
2.5 Mg	12.0 <sup>c</sup>	40.4 <sup>d</sup>	9.9 <sup>d</sup>	7.9 <sup>b</sup>	21.9 <sup>e</sup>
5.0 Mg	10.8 <sup>a</sup>	37.5 <sup>b</sup>	13.3 <sup>c</sup>	9.4 <sup>e</sup>	19.2 <sup>ab</sup>
10.0 Mg	8.4 <sup>d</sup>	40.4 <sup>d</sup>	14.7 <sup>a</sup>	8.9 <sup>c</sup>	15.1 <sup>cd</sup>
$\kappa$ -casein					
0	12.6 <sup>a</sup>	32.6 <sup>a</sup>	10.7 <sup>a</sup>	10.8 <sup>a</sup>	21.8 <sup>a</sup>
2.5 Ca	12.7 <sup>a</sup>	44.2 <sup>b</sup>	11.1 <sup>ab</sup>	8.2 <sup>b</sup>	14.7 <sup>b</sup>
5.0 Ca	9.6 <sup>bc</sup>	38.0 <sup>c</sup>	9.2 <sup>c</sup>	9.7 <sup>c</sup>	21.5 <sup>c</sup>
10.0 Ca	9.3 <sup>c</sup>	42.3 <sup>d</sup>	14.7 <sup>d</sup>	8.6 <sup>d</sup>	12.6 <sup>d</sup>
2.5 Mg	10.5 <sup>d</sup>	44.3 <sup>b</sup>	9.8 <sup>e</sup>	9.2 <sup>e</sup>	16.9 <sup>e</sup>
5.0 Mg	9.8 <sup>b</sup>	40.1 <sup>e</sup>	11.3 <sup>b</sup>	10.0 <sup>f</sup>	19.6 <sup>f</sup>
10.0 Mg	8.9 <sup>e</sup>	43.1 <sup>f</sup>	13.15 <sup>f</sup>	8.8 <sup>g</sup>	14.8 <sup>g</sup>

<sup>a</sup> Casein concentration, 10 mg mL<sup>-1</sup>. Values are means (n = 2); means in the same column for a specific casein that do not share the same small letters differ significantly (P < 0.05). Wavenumbers are:  $\alpha$ -helices, 1651–1653 cm<sup>-1</sup>; total  $\beta$ -sheet, 1619–1642 and 1688–1697 cm<sup>-1</sup>; random, 1644–1648 cm<sup>-1</sup>;  $3_{10}$ -helix, 1661–1664 cm<sup>-1</sup>;  $\beta$ -turns, 1667–1678 cm<sup>-1</sup>.

Wickham, Piotrowski, Fagerquist, & Farrell, 2005), which suggested 7–25%  $\alpha$ -helix and 15–33%  $\beta$ -sheet.  $\kappa$ -CN with an  $\alpha$ -helical structure of 13%, 33%  $\beta$ -sheet and 22% turns are in agreement with previous estimates that it may contain 10–20%  $\alpha$ -helix, 20–30%  $\beta$ -structure and 15–25% turns (Kumosinski, Brown, & Farrell, 1991, 1993; Byler & Susi, 1986; Farrell et al., 1996; Ono, Yada, Yutani, & Nakai, 1987). However, the estimated secondary structures in the current study differed from some of the previous reports based on far-UV CD NMR, FTIR (Alaimo, Farrell, & Germann, 1999) and Raman spectroscopy (Byler et al., 1988), possibly due to different band assignments. Predicted secondary structure of both  $\beta$ -CN and  $\kappa$ -CN are different from  $\alpha_{S1}$ -CN and  $\alpha_{S2}$ -CN and could be due to their distinct polar and hydrophobic domains and monomer-polymer micelle self-association equilibria compared with consecutive self-association observed in  $\alpha_{S1}$ -CN. Differences in  $\beta$ -CN and  $\kappa$ -CN could be due to the former being more hydrophobic and thus its self-association being highly temperature-dependent.

### 3.2. Secondary structure of binary mixtures of caseins

Only few studies have reported mixed associations involving primary binary mixtures (mainly  $\alpha_{S1}$ -CN +  $\beta$ -CN,  $\alpha_{S1}$ -CN +  $\kappa$ -CN and  $\beta$ -CN +  $\kappa$ -CN) and that too on the weight average molecular weight of protomers and apparent association constants by analytical centrifugation (Farrell et al., 2013). Caseins change significantly in their secondary structure when present with another casein as demonstrated by curve fitting (Table 1). Compared with conformation of individual caseins,  $\alpha_{S1}$ -CN in a binary mixture with other caseins exhibited a decrease in random,  $\alpha$ -helix (except with  $\beta$ -CN),  $\beta$ -sheet (except with  $\alpha_{S2}$ -CN) and triple

helices and increase in turns in presence of another casein.  $\alpha_{S2}$ -CN in a binary mixture with another casein showed no significant change in turns, a decrease in  $\alpha$ -helix, random and triple helices and an increase in level of  $\beta$ -sheet (except with  $\beta$ -CN).  $\beta$ -CN in a binary mixture with  $\alpha_{S2}$ -CN and  $\kappa$ -CN had significantly lower levels of  $\alpha$ -helix, random and triple ( $3_{10}$ ) helix and higher amount of  $\beta$ -sheet and  $\beta$ -turns (Table 1). However, in a binary mixture with  $\alpha_{S1}$ -CN,  $\beta$ -CN had higher  $\alpha$ -helix and  $\beta$ -sheet at expense of random and triple helix structures.  $\kappa$ -CN in a mixture had higher  $\beta$ -sheet and triple helices (except no difference when with  $\alpha_{S2}$ -CN) and lower  $\alpha$ -helix (except no difference when with  $\alpha_{S1}$ -CN) and  $\beta$ -turns (except no difference when with  $\alpha_{S2}$ -CN).

A very interesting feature noted was that the secondary structure of the binary mixture was not the average of the constituent individual caseins. For all the combinations, the presence of another casein in a binary mixture was marked by an increase in  $\beta$ -sheet (except  $\alpha_{S1}$ -CN +  $\kappa$ -CN mixture) and  $\beta$ -turns at the expense of  $\alpha$ -helix (except  $\alpha_{S1}$ -CN +  $\beta$ -CN mixture), triple helix and random structures when compared with the average of the individual caseins at the given ratio. PCA score plot further demonstrated that a particular casein in a binary mixture with other casein engages in protein-protein interactions leading to significant changes in their conformation (Fig. 1). Binary mixtures of  $\alpha_{S2}$ -,  $\beta$ - and  $\kappa$ -CN were separated from other individual caseins and  $\alpha_{S1}$ -CN mixtures along PC 3, with a high positive loading for  $\alpha$ -helix structures and PC 2 with high negative loading for  $\beta$ -sheet (Fig. 1).

Increase in sheet and turn structures implies an important role of intermolecular  $\beta$ -sheets and turns or sheet-turn-sheet motifs in inter-casein interactions. Considering increase in turns, hydrophobic interactions appear to play a key role. However,  $\beta$ -sheet is

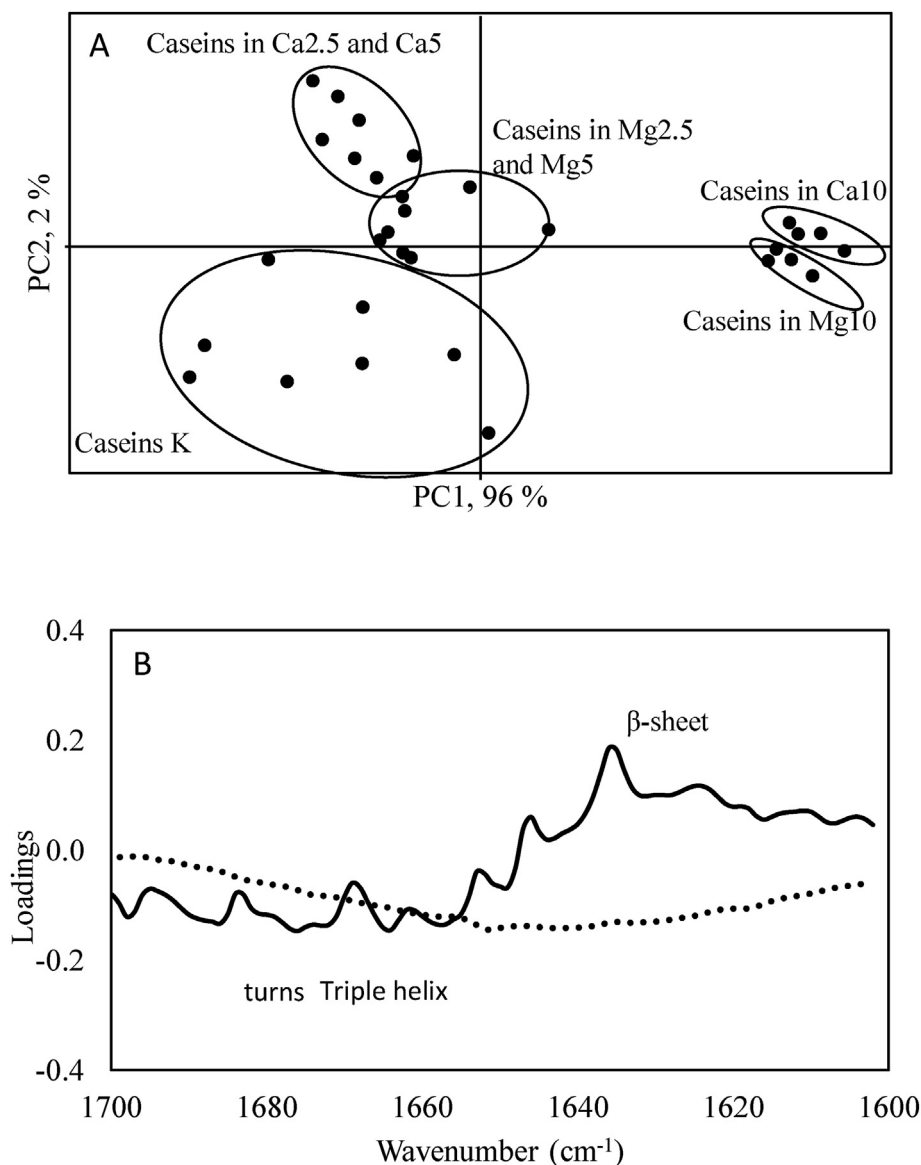


**Fig. 2.** PCA plot (A) with loadings (B; .....; PC1; —, PC2) of FTIR data in the region 1700–1600  $\text{cm}^{-1}$  for individual caseins in PIPES buffer (10  $\text{mg mL}^{-1}$ ) without (K) or with Ca or Mg at different concentrations of 2.5  $\text{mmol L}^{-1}$  (Ca2.5; Mg2.5), 5  $\text{mmol L}^{-1}$  (Ca5; Mg5) or 10  $\text{mmol L}^{-1}$  (Ca10; Mg10).

also strongly driven by hydrogen bonding, and hence this would cast some doubt on hydrophobic interactions being the only factor. This is also consistent with the views that the backbone of the peptide chain, rather than the side-groups, have a very high importance in casein interactions (Holt et al., 2013). The increase in  $\beta$ -sheet and turn structures supports the proposed tensegrity structural analogy that casein–casein interactions occur primarily via sheet–turn–sheet interactions (Farrell et al., 2013). In addition, the segregation of  $\alpha_{S1}$ -CN and its mixtures as a separate group in PCA (Fig. 1) could be explained by the hypothesis proposed by Farrell et al. (2013) that considered  $\alpha_{S1}$ -CN as the natively unfolded assembler able to breakdown self-associated aggregates or amyloid bodies of other caseins, and thus acting as a primary force in casein micelle secretion.  $\alpha_{S1}$ -CN also definitely induces markedly different changes in conformation (high  $\beta$ -sheet structures) when present in a binary mixture with another casein. Marked decreases in helical structures in binary mixtures without  $\alpha_{S1}$ -CN indicate a different type of protein–protein interaction. The loop–helix–loop regions were probably playing predominant role in these mixtures.

### 3.3. Influence of $\text{Ca}^{2+}$ and $\text{Mg}^{2+}$ on the secondary structure of individual caseins

The presence of  $\text{Ca}^{2+}$  or  $\text{Mg}^{2+}$  cations in the buffer induced significant changes in the secondary structure of individual caseins. Concentrations of  $\text{Ca}^{2+}$  and  $\text{Mg}^{2+}$  were chosen to represent calcium concentrations representative for the serum phase of milk (approximately 10  $\text{mmol L}^{-1}$ ), and also for cation:casein ratios encountered in, e.g., calcium caseinate and magnesium caseinate. Curve fitting clearly showed an increase in  $\beta$ -sheet structure and a decline in triple helices and  $\beta$ -turns (only exception being increase in turns in  $\alpha_{S1}$ -CN) when  $\text{Ca}^{2+}$  and  $\text{Mg}^{2+}$  ion was added (Table 2). However, addition of  $\text{Mg}^{2+}$  resulted in a lower degree of changes in secondary structure compared with  $\text{Ca}^{2+}$ . Furthermore, increases in concentration of  $\text{Ca}^{2+}$  and  $\text{Mg}^{2+}$  ion in the buffer produced different effects depending on the type of casein and cation.

Increased concentration of Ca resulted in a decrease in  $\alpha$ -helix (not in  $\alpha_{S1}$ -CN and  $\alpha_{S2}$ -CN),  $\beta$ -sheet and turns, and an increase in random and triple helices (except in  $\alpha_{S1}$ -CN). The changes in

**Table 3**  
Percentage areas of different secondary structures in amide I for binary mixture of  $\alpha_{S1}$ -casein,  $\alpha_{S2}$ -casein,  $\beta$ -casein and  $\kappa$ -casein in PIPES buffer without or with Ca or Mg.<sup>a</sup>

Added Ca or Mg (mM)	$\alpha$ -helix	Total $\beta$ -sheet	Random	$3_{10}$ -helix	Total $\beta$ -turns
$\alpha_{S1}$ -casein + $\kappa$ -casein (4:1)					
0	12.8 <sup>a</sup>	34.1 <sup>a</sup>	11.8 <sup>ab</sup>	12.0 <sup>a</sup>	20.4 <sup>a</sup>
2.5 Ca	12.0 <sup>a</sup>	44.1 <sup>b</sup>	11.1 <sup>a</sup>	8.5 <sup>b</sup>	15.6 <sup>cd</sup>
5.0 Ca	11.9 <sup>a</sup>	40.2 <sup>d</sup>	11.8 <sup>ab</sup>	9.5 <sup>bc</sup>	17.2 <sup>bc</sup>
10.0 Ca	9.0 <sup>b</sup>	41.7 <sup>c</sup>	13.5 <sup>b</sup>	9.8 <sup>bc</sup>	13.2 <sup>d</sup>
2.5 Mg	8.5 <sup>b</sup>	42.1 <sup>c</sup>	11.7 <sup>ab</sup>	10.1 <sup>bc</sup>	19.7 <sup>ab</sup>
5.0 Mg	9.5 <sup>b</sup>	39.9 <sup>d</sup>	12.2 <sup>ab</sup>	10.3 <sup>ac</sup>	20.3 <sup>a</sup>
10.0 Mg	9.6 <sup>b</sup>	38.1 <sup>e</sup>	10.2 <sup>a</sup>	9.3 <sup>bc</sup>	22.4 <sup>a</sup>
$\beta$ -casein + $\kappa$ -casein (4:1)					
0	9.9 <sup>a</sup>	40.1 <sup>a</sup>	11.0 <sup>ab</sup>	12.0 <sup>a</sup>	20.4 <sup>a</sup>
2.5 Ca	11.3 <sup>b</sup>	46.6 <sup>b</sup>	10.8 <sup>bc</sup>	8.5 <sup>bc</sup>	12.7 <sup>b</sup>
5.0 Ca	10.4 <sup>c</sup>	40.6 <sup>c</sup>	10.8 <sup>bc</sup>	8.8 <sup>b</sup>	16.5 <sup>c</sup>
10.0 Ca	12.2 <sup>d</sup>	42.4 <sup>d</sup>	6.2 <sup>d</sup>	6.0 <sup>f</sup>	20.1 <sup>d</sup>
2.5 Mg	8.8 <sup>e</sup>	40.6 <sup>c</sup>	11.5 <sup>a</sup>	10.1 <sup>e</sup>	19.4 <sup>e</sup>
5.0 Mg	10.5 <sup>c</sup>	42.1 <sup>e</sup>	10.4 <sup>c</sup>	9.5 <sup>d</sup>	17.9 <sup>f</sup>
10.0 Mg	10.1 <sup>ac</sup>	43.2 <sup>f</sup>	12.2 <sup>e</sup>	9.2 <sup>cd</sup>	16.2 <sup>g</sup>
$\alpha_{S2}$ -casein + $\kappa$ -casein (1:1)					
0	9.6 <sup>b</sup>	40.2 <sup>a</sup>	10.6 <sup>a</sup>	11.8 <sup>a</sup>	21.2 <sup>a</sup>
2.5 Ca	11.1 <sup>c</sup>	45.9 <sup>b</sup>	11.3 <sup>a</sup>	8.5 <sup>b</sup>	14.8 <sup>b</sup>
5.0 Ca	10.2 <sup>bc</sup>	40.5 <sup>a</sup>	11.5 <sup>ab</sup>	8.8 <sup>b</sup>	15.6 <sup>c</sup>
10.0 Ca	9.5 <sup>b</sup>	41.5 <sup>a</sup>	13.6 <sup>b</sup>	8.7 <sup>b</sup>	13.1 <sup>d</sup>
2.5 Mg	10.2 <sup>bc</sup>	41.5 <sup>a</sup>	11.3 <sup>ab</sup>	10.1 <sup>d</sup>	19.5 <sup>e</sup>
5.0 Mg	8.1 <sup>a</sup>	40.6 <sup>a</sup>	11.5 <sup>ab</sup>	10.1 <sup>d</sup>	21.8 <sup>f</sup>
10.0 Mg	8.9 <sup>ab</sup>	39.1 <sup>a</sup>	12.4 <sup>ab</sup>	9.5 <sup>cd</sup>	16.3 <sup>g</sup>
$\alpha_{S1}$ -casein + $\alpha_{S2}$ -casein (4:1)					
0	10.3 <sup>ad</sup>	39.6 <sup>a</sup>	10.5 <sup>a</sup>	12.5 <sup>a</sup>	20.2 <sup>a</sup>
2.5 Ca	12.7 <sup>b</sup>	48.2 <sup>b</sup>	10.7 <sup>ab</sup>	8.9 <sup>bc</sup>	11.9 <sup>b</sup>
5.0 Ca	12.3 <sup>b</sup>	44.6 <sup>c</sup>	9.7 <sup>a</sup>	8.3 <sup>b</sup>	17.2 <sup>acd</sup>
10.0 Ca	8.5 <sup>c</sup>	41.4 <sup>ac</sup>	14.3 <sup>c</sup>	9.4 <sup>bcd</sup>	14.2 <sup>bc</sup>
2.5 Mg	11.4 <sup>bd</sup>	41.5 <sup>ac</sup>	10.5 <sup>a</sup>	10.1 <sup>d</sup>	20.0 <sup>a</sup>
5.0 Mg	10.3 <sup>ad</sup>	44.1 <sup>c</sup>	10.3 <sup>a</sup>	10.1 <sup>d</sup>	19.0 <sup>ad</sup>
10.0 Mg	9.8 <sup>a</sup>	43.5 <sup>c</sup>	12.1 <sup>b</sup>	9.7 <sup>cd</sup>	16.6 <sup>cd</sup>
$\alpha_{S1}$ -casein + $\beta$ -casein (1:1)					
0	14.8 <sup>a</sup>	36.9 <sup>a</sup>	11.3 <sup>ab</sup>	11.2 <sup>a</sup>	18.9 <sup>a</sup>
2.5 Ca	11.6 <sup>b</sup>	44.0 <sup>b</sup>	10.2 <sup>b</sup>	8.7 <sup>b</sup>	16.8 <sup>b</sup>
5.0 Ca	12.0 <sup>b</sup>	43.8 <sup>b</sup>	10.2 <sup>b</sup>	8.4 <sup>bc</sup>	15.7 <sup>c</sup>
10.0 Ca	10.3 <sup>c</sup>	43.0 <sup>b</sup>	12.3 <sup>a</sup>	8.0 <sup>c</sup>	14.4 <sup>d</sup>
2.5 Mg	9.8 <sup>c</sup>	43.8 <sup>b</sup>	11.4 <sup>ab</sup>	8.8 <sup>b</sup>	18.3 <sup>e</sup>
5.0 Mg	10.0 <sup>c</sup>	40.8 <sup>c</sup>	11.4 <sup>ab</sup>	10.3 <sup>d</sup>	19.5 <sup>f</sup>
10.0 Mg	8.3 <sup>d</sup>	35.7 <sup>a</sup>	11.7 <sup>a</sup>	10.0 <sup>d</sup>	20.3 <sup>g</sup>
$\beta$ -casein + $\alpha_{S2}$ -casein (4:1)					
0	9.8 <sup>a</sup>	33.2 <sup>a</sup>	10.0 <sup>ab</sup>	11.3 <sup>a</sup>	20.4 <sup>a</sup>
2.5 Ca	11.3 <sup>a</sup>	36.0 <sup>ab</sup>	9.9 <sup>ab</sup>	8.4 <sup>bd</sup>	24.4 <sup>b</sup>
5.0 Ca	10.3 <sup>a</sup>	40.6 <sup>ab</sup>	11.0 <sup>ab</sup>	9.2 <sup>bcd</sup>	18.2 <sup>c</sup>
10.0 Ca	9.2 <sup>a</sup>	41.8 <sup>b</sup>	12.4 <sup>b</sup>	7.8 <sup>d</sup>	15.2 <sup>d</sup>
2.5 Mg	8.9 <sup>a</sup>	40.8 <sup>ab</sup>	11.8 <sup>b</sup>	9.7 <sup>abc</sup>	17.8 <sup>e</sup>
5.0 Mg	9.8 <sup>a</sup>	40.5 <sup>ab</sup>	11.3 <sup>b</sup>	10.3 <sup>ac</sup>	20.0 <sup>f</sup>
10.0 Mg	8.8 <sup>a</sup>	35.9 <sup>ab</sup>	7.6 <sup>a</sup>	7.5 <sup>d</sup>	22.6 <sup>g</sup>

<sup>a</sup> Total casein concentration 10 mg mL<sup>-1</sup>, mixture ratio indicated between brackets. Values are means (n = 2); means in the same column for a specific casein mixture that do not share the same small letters differ significantly (P < 0.05). Wavenumbers are:  $\alpha$ -helices, 1651–1653 cm<sup>-1</sup>; total  $\beta$ -sheet, 1619–1642 and 1688–1697 cm<sup>-1</sup>; random, 1644–1648 cm<sup>-1</sup>;  $3_{10}$ -helix, 1661–1664 cm<sup>-1</sup>;  $\beta$ -turns, 1667–1678 cm<sup>-1</sup>.

secondary structure with increase in concentration of Mg was quite variable. With increasing Mg, there was a decrease in  $\alpha$ -helix (except an increase in  $\alpha_{S2}$ -CN),  $\beta$ -sheet (no change in  $\beta$ -CN and an increase in  $\alpha_{S2}$ -CN), turns (except in  $\alpha_{S1}$ -CN and  $\beta$ -CN) and an increase in random (except in  $\beta$ -CN) and triple helices (except in  $\alpha_{S2}$ -CN and  $\kappa$ -CN). Thus, the presence of the divalent cations Ca<sup>2+</sup> and Mg<sup>2+</sup> in solutions of individual caseins significantly impacted their secondary structure (Fig. 2). In contrast to a previous report (Ono, Yahagi, & Odagiri, 1980), the binding of calcium to  $\kappa$ -CN also induced significant changes in the secondary structure of the protein. PCA further supported curve fitting results as caseins in presence of Ca and Mg cations were classified as separate groups (Fig. 2). According to the loading plot of PC2, a high loading for  $\beta$ -sheet and a low loading for turns and helices was observed. Comparing the samples containing Ca<sup>2+</sup> and Mg<sup>2+</sup>, the former had a higher loading for  $\beta$ -sheet while the latter had higher loading for

$\beta$ -turns. This explained the comparatively lower modification in secondary structures of caseins in presence of Mg than in the presence of Ca.

Ca<sup>2+</sup> binds to recurrent and phosphorylated loop-helix loop regions in caseins, which could deform these elements (Holt et al., 1993; Kumosinski & Farrell, 1994). Different studies on interactions of individual caseins with Ca<sup>2+</sup> have revealed that the driving forces behind the calcium-induced interactions are hydrogen bonding and hydrophobic interactions in the absence of electrostatic repulsion (Dagleish & Parker, 1980; Ono et al., 1980; Ono, Kaminogawa, Odagiri, & Yamauchi, 1976). No calcium-induced cross-linkage of proteins occurs as calcium-induced precipitates are readily solubilised in 4 M urea (Aoki, Toyooka, & Kako, 1985). Hydrophobic regions of caseins have sheet-turn-sheet motifs and thus the increases observed in  $\beta$ -sheet structures in this study on introduction of Ca<sup>2+</sup> in buffer solutions could be due to these interactions.

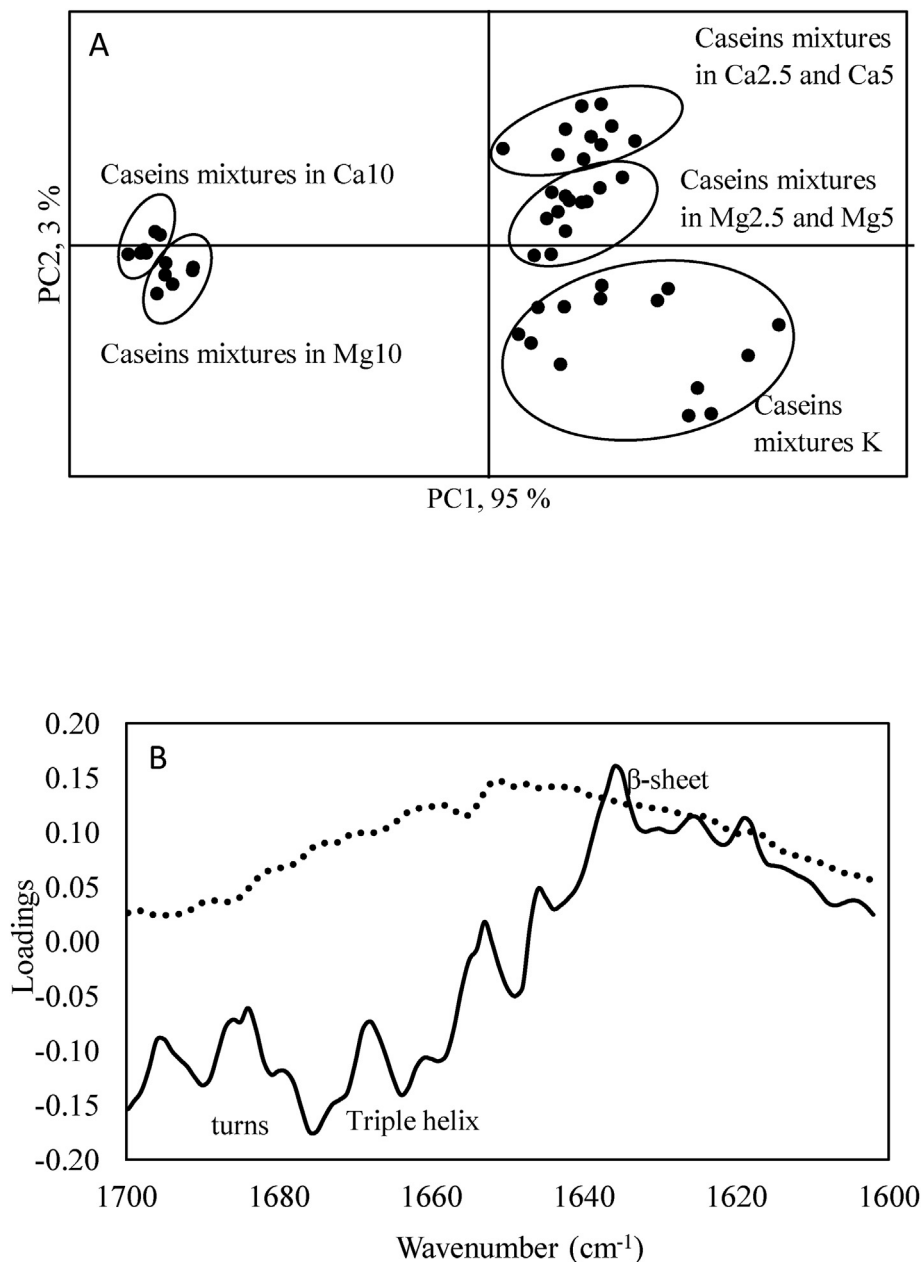


**Fig. 3.** PCA plot (A) with loadings (B; .....; PC1; —, PC2) of FTIR data in the region 1700–1600  $\text{cm}^{-1}$  for binary mixtures of caseins in a ratio of 1:1 ( $\alpha_{S1}$ -CN +  $\beta$ -CN;  $\alpha_{S2}$ -CN +  $\kappa$ -CN) or 4:1 ( $\alpha_{S1}$ -CN +  $\alpha_{S2}$ -CN;  $\alpha_{S1}$ -CN +  $\kappa$ -CN;  $\beta$ -CN +  $\alpha_{S2}$ -CN;  $\beta$ -CN +  $\kappa$ -CN) in PIPES buffer without (K) or with Ca or Mg at different concentrations of 2.5  $\text{mmol L}^{-1}$  (Ca2.5; Mg2.5), 5  $\text{mmol L}^{-1}$  (Ca5; Mg5) or 10  $\text{mmol L}^{-1}$  (Ca10; Mg10).

Moreover, the agreed preferential binding of  $\text{Ca}^{2+}$  to high-affinity phosphoserine clusters present in loop-helix-loop motifs in the polar domains of caseins could also explain loss of helical element. Binding of  $\text{Ca}^{2+}$  to phosphoserine clusters in the polar domain is also suggested to alter its interaction with the hydrophobic domain, bringing about a conformational change in that domain resulting in some associations expressed as increase in sheet structures. Further,  $\text{Ca}^{2+}$  reportedly also binds to carboxylate-containing residues (Asp and Glu) throughout the structure reducing the electrostatic repulsion and, consequently, enhanced interaction of the hydrophobic domains (Huppertz, 2013). Previously, the contribution of carboxylate residues to  $\text{Ca}^{2+}$ -binding capacity was assumed to be small due to decrease in  $\text{Ca}^{2+}$  binding

to dephosphorylated caseins (Dickson & Perkins, 1971). However, a recent study (Bijl et al., 2018) suggested that approximately 1 in 5 of Glu and Asp residues bind a Ca ion. Those authors calculated that approximately one carboxyl group is involved in sequestration of the nanoclusters for every casein phosphate moiety, e.g.,  $\beta$ -CN with 5 phosphate groups contributes 5 out of its total of 24 carboxyl groups to the sequestration reaction.

Introduction of  $\text{Mg}^{2+}$  into the buffer containing individual caseins also induced significant changes in their secondary structure though comparatively to a less extent as compared with the effect of  $\text{Ca}^{2+}$ . Less effect of  $\text{Mg}^{2+}$  ion could be due to comparatively lower affinity of caseins for this ion compared with  $\text{Ca}^{2+}$  (Philippe, Le Graët, & Gaucheron, 2005). The presence of  $\text{Mg}^{2+}$  also resulted in

an increase in  $\beta$ -sheet structures and reduction in triple helix. However, addition of  $Mg^{2+}$  did not reduce turns to an extent as with  $Ca^{2+}$ . As compared with the numerous studies on interactions of  $Ca^{2+}$  with caseins, there has been hardly any study elaborating on the influence of  $Mg^{2+}$  on conformational changes of individual caseins.  $Mg^{2+}$  probably also binds to phosphate residues and carboxylate-containing residues (Asp and Glu) in polar domains of the structure, minimising the electrostatic repulsion and hence increasing hydrophobic interaction via sheet-turn-sheet motifs. This explains the observed increase in  $\beta$ -sheet structures. Deformation of triple helical components could be explained by the tensegrity hypothesis of Farrell et al. (2013), which proposes that flexible loop-helix-loop motifs in the structure are subject to conformational change on binding of ligands.

### 3.4. Influence of Ca and Mg on the secondary structure of binary mixtures of caseins

The presence of  $Ca^{2+}$  and  $Mg^{2+}$  in binary mixtures of caseins significantly impacted their secondary structure in a somewhat similar way as individual caseins. Addition of Ca and Mg in binary mixtures resulted in an increase in  $\beta$ -sheet (except  $\alpha_{S2}$ -CN +  $\kappa$ -CN mixtures) and decrease in triple helix and  $\beta$ -turns. In contrast to individual caseins, in presence of Ca some binary mixtures exhibited an increase in  $\alpha$  helix and random. Like individual caseins, on addition of  $Mg^{2+}$  ion, there was either a decrease or no change in  $\alpha$  helix (except an increase in  $\beta$ -CN +  $\kappa$ -CN mixture) and random structures (except an increase in mixture  $\beta$ -CN +  $\kappa$ -CN and  $\alpha_{S1}$ -CN +  $\alpha_{S2}$ -CN) (Tables 2 and 3). Less effect of  $Mg^{2+}$  ion could be due to comparatively lower affinity of caseins to the ion compared with  $Ca^{2+}$  (Philippe et al., 2005).

Increased concentration of Ca resulted in a decrease in  $\alpha$ -helix (not in the  $\beta$ -CN +  $\kappa$ -CN mixture),  $\beta$ -sheet triple, helix and turns (except in the  $\beta$ -CN +  $\kappa$ -CN mixture) and an increase in random (except in the  $\beta$ -CN +  $\kappa$ -CN mixture). As observed previously, increased  $Mg^{2+}$  concentration did not alter significantly structural features in many of the binary mixtures. Generally, with higher Mg concentration, a decrease in  $\alpha$ -helix (except an increase in the  $\beta$ -CN +  $\kappa$ -CN mixture),  $\beta$ -sheet (except in the  $\beta$ -CN +  $\kappa$ -CN mixture), turns (except in the  $\alpha_{S1}$ -CN,  $\alpha_{S2}$ -CN and  $\beta$ -CN binary mixtures) and an increase in random (except in the mixture of  $\alpha_{S2}$ -CN +  $\beta$ -CN) and triple helices was observed (Tables 2 and 3). PCA results in Fig. 3 also demonstrated that both Ca and Mg had significant effect on secondary structure of binary mixtures. The score plots further revealed that there were also subtle differences between the effects of Ca and Mg. Furthermore, as discussed in the previous paragraph, the concentration of Ca and Mg in the buffer also had a significant effect.

The results agree with those of Curley et al. (1998), who reported that the addition of  $Ca^{2+}$  in salt solutions ( $Na^+$  or  $K^+$ ) of sodium caseinate resulted in decrease in large loop or helical structures. However, in contrast to their reports, in our study, a decrease in helical structures was not associated with an increase in turns, probably due to dissimilar band assignments.

## 4. Conclusion

The present study, for the first time, has presented quantification of changes in secondary structure of individual milk caseins when present in a binary mixture with another casein with or without  $Ca^{2+}$  or  $Mg^{2+}$ . The curve fitting and assignment results provided measure for changes in secondary structure on modification in their environment. PCA analysis augmented the results further. Both for individual caseins and their binary mixtures, addition of Ca and Mg resulted in increase in  $\beta$ -sheet structures and

decrease in triple helices and turns, implying binding of cations to similar sites. Binding of cations with phosphoserine clusters with loop-helix-loop motifs explained the reduction in the helical element. In addition, the binding of cations to electronegative regions reduced electrostatic repulsion, resulting in an increase in hydrophobic interactions, thus explaining the increase in sheet structures. The only difference in changes in secondary structure of individual caseins and binary mixtures in the presence of either Ca/Mg was an increase in random structures in the latter. In addition, compared with Mg ions, it seemed that Ca had more affinity for caseins, especially when they were in a binary mixture.

## References

- Alaimo, M. H., Farrell, H. M., & Germann, M. W. (1999). Conformational analysis of the hydrophobic peptide  $\alpha_{S1}$ -casein(136–196). *Biochimica et Biophysica Acta (BBA) - Protein Structure and Molecular Enzymology*, 1431, 410–420.
- Aoki, T., Toyooka, K., & Kako, Y. (1985). Role of phosphate groups in the calcium sensitivity of  $\alpha_{S2}$ -casein. *Journal of Dairy Science*, 68, 1624–1629.
- Bijl, E., Huppertz, T., van Valenberg, H., & Holt, C. (2018). A quantitative model of the bovine casein micelle: Ion equilibria and calcium phosphate sequestration by individual caseins in bovine milk. *European Biophysics Journal*, 48, 45–59.
- Byler, D. M., & Farrell, H. M. (1989). Infrared spectroscopic evidence for calcium ion interaction with carboxylate groups of casein. *Journal of Dairy Science*, 72, 1719–1723.
- Byler, D. M., Farrell, H. M., & Susi, H. (1988). Raman spectroscopic study of casein structure. *Journal of Dairy Science*, 71, 2622–2629.
- Byler, D. M., & Susi, H. (1986). Examination of the secondary structure of proteins by deconvolved FTIR spectra. *Biopolymers: Original Research on Biomolecules*, 25, 469–487.
- Creamer, L., Richardson, T., & Parry, D. (1981). Secondary structure of bovine  $\alpha_{S1}$ - and  $\beta$ -casein in solution. *Archives of Biochemistry and Biophysics*, 211, 689–696.
- Curley, D. M., Kumosinski, T. F., Unruh, J. J., & Farrell, H. M. (1998). Changes in the secondary structure of bovine casein by Fourier transform infrared spectroscopy: Effects of calcium and temperature. *Journal of Dairy Science*, 81, 3154–3162.
- Dalgleish, D. G., & Parker, T. G. (1980). Binding of calcium ions to bovine  $\alpha_{S1}$ -casein and precipitability of the protein–calcium ion complexes. *Journal of Dairy Research*, 47, 113–122.
- Dickson, I., & Perkins, D. (1971). Studies on the interactions between purified bovine caseins and alkaline-earth-metal ions. *Biochemical Journal*, 124, 235–240.
- Farrell, H. M., Brown, E. M., Hoagland, P. D., & Malin, E. L. (2003). Higher order structures of the caseins: A paradox? In P. L. H. McSweeney, & P. F. Fox (Eds.), *Advanced dairy chemistry. Vol. 1. Proteins* (3<sup>rd</sup> ed., pp. 203–231). Boston, MA, USA: Springer US.
- Farrell, H. M., Brown, E. M., & Malin, E. L. (2013). Higher order structures of the caseins: A paradox? In P. L. H. McSweeney, & P. F. Fox (Eds.), *Advanced dairy chemistry. Vol. 1A. Proteins: Basic aspects* (4<sup>th</sup> ed., pp. 161–184). Boston, MA, USA: Springer US.
- Farrell, H. M., Kumosinski, T. F., Cooke, P. H., King, G., Hoagland, P. D., Wickham, E. D., et al. (1996). Particle sizes of purified  $\kappa$ -casein: Metal effect and correspondence with predicted three-dimensional molecular models. *Journal of Protein Chemistry*, 15, 435–445.
- Farrell, H. M., Wickham, E. D., Unruh, J. J., Qi, P. X., & Hoagland, P. D. (2001). Secondary structural studies of bovine caseins: Temperature dependence of  $\beta$ -casein structure as analyzed by circular dichroism and FTIR spectroscopy and correlation with micellization. *Food Hydrocolloids*, 15, 341–354.
- Goldberg, M. E., & Chaffotte, A. F. (2005). Undistorted structural analysis of soluble proteins by attenuated total reflectance infrared spectroscopy. *Protein Science*, 14, 2781–2792.
- Grewal, M. K., Chandrapala, J., Donkor, O., Apostolopoulos, V., Stojanovska, L., & Vasiljevic, T. (2017). Fourier transform infrared spectroscopy analysis of physicochemical changes in UHT milk during accelerated storage. *International Dairy Journal*, 66, 99–107.
- Grewal, M. K., Huppertz, T., & Vasiljevic, T. (2018). FTIR fingerprinting of structural changes of milk proteins induced by heat treatment, deamidation and dephosphorylation. *Food Hydrocolloids*, 80, 160–167.
- Hoagland, P., Unruh, J., Wickham, E., & Farrell, H. (2001). Secondary structure of bovine  $\alpha_{S2}$ -casein: Theoretical and experimental approaches. *Journal of Dairy Science*, 84, 1944–1949.
- Holt, C., Carver, J., Ecrolyd, H., & Thorn, D. (2013). Invited review: Caseins and the casein micelle: Their biological functions, structures, and behavior in foods. *Journal of Dairy Science*, 96, 6127–6146.
- Holt, C., & Sawyer, L. (1993). Caseins as rheomorphic proteins: Interpretation of primary and secondary structures of the  $\alpha_{S1}$ -,  $\beta$ - and  $\kappa$ -caseins. *Journal of the Chemical Society, Faraday Transactions*, 89, 2683–2692.
- Huppertz, T. (2013). Chemistry of the caseins. In P. L. H. McSweeney, & P. F. Fox (Eds.), *Advanced dairy chemistry. Vol. 1A. Proteins: Basic aspects* (4<sup>th</sup> ed., pp. 135–160). Boston, MA, USA: Springer US.

- Huppertz, T., Fox, P. F., & Kelly, A. L. (2018). The caseins: Structure, stability, and functionality. In R. Y. Yada (Ed.), *Proteins in food processing* (2<sup>nd</sup> ed., pp. 49–92). Cambridge, UK: Woodhead Publishing.
- Kakalis, L. T., Kumosinski, T. F., & Farrell, H. M. (1990). A multinuclear, high-resolution NMR study of bovine casein micelles and submicelles. *Biophysical Chemistry*, 38, 87–98.
- Kumosinski, T., Brown, E., & Farrell, H. (1991). Three-dimensional molecular modeling of bovine caseins:  $\alpha_{S1}$ -casein. *Journal of Dairy Science*, 74, 2889–2895.
- Kumosinski, T. F., Brown, E. M., & Farrell, H. M. (1993). Three-dimensional molecular modeling of bovine caseins: An energy-minimized  $\beta$ -casein structure. *Journal of Dairy Science*, 76, 931–945.
- Kumosinski, T. F., & Farrell, H. M., Jr. (1994). *Solubility of proteins: Protein-saltwater interactions*. New York, NY, USA: Marcel Dekker, Inc.
- Leaver, J., & Law, A. J. (1992). Preparative-scale purification of bovine caseins on a cation-exchange resin. *Journal of Dairy Research*, 59, 557–561.
- Malin, E. L., Brown, E. M., Wickham, E. D., & Farrell, H. M. (2005). Contributions of terminal peptides to the associative behavior of  $\alpha_{S1}$ -casein. *Journal of Dairy Science*, 88, 2318–2328.
- Mulvihill, D., & Fox, P. (1977). Proteolysis of  $\alpha_{S1}$ -casein by chymosin: Influence of pH and urea. *Journal of Dairy Research*, 44, 533–540.
- Ono, T., Kaminogawa, S., Odagiri, S., & Yamauchi, K. (1976). A study on the binding of calcium ions to  $\alpha_{S1}$ -casein. *Agricultural & Biological Chemistry*, 40, 1717–1723.
- Ono, T., Yada, R., Yutani, K., & Nakai, S. (1987). Comparison of conformations of  $\kappa$ -casein, para- $\kappa$ -casein and glycomacropeptide. *Biochimica et Biophysica Acta (BBA) - Protein Structure and Molecular Enzymology*, 911, 318–325.
- Ono, T., Yahagi, M., & Odagiri, S. (1980). The binding of calcium to  $\kappa$ -casein and para  $\kappa$ -casein. *Agricultural & Biological Chemistry*, 44, 1499–1503.
- Philippe, M., Le Graët, Y., & Gaucheron, F. (2005). The effects of different cations on the physicochemical characteristics of casein micelles. *Food Chemistry*, 90, 673–683.
- Qi, P. X., Wickham, E. D., & Farrell, H. M. (2004). Thermal and alkaline denaturation of bovine  $\beta$ -casein. *The Protein Journal*, 23, 389–402.
- Qi, P. X., Wickham, E. D., Piotrowski, E. G., Fagerquist, C. K., & Farrell, H. M. (2005). Implication of C-terminal deletion on the structure and stability of bovine  $\beta$ -casein. *The Protein Journal*, 24, 431–444.
- Sawyer, L., Barlow, P. N., Boland, M. J., Creamer, L. K., Denton, H., Edwards, P. J. B., et al. (2002). Milk protein structure—what can it tell the dairy industry? *International Dairy Journal*, 12, 299–310.
- Snoeren, T., Van Der Spek, C., & Payens, T. (1977). Preparation of  $\kappa$ -and minor  $\alpha$ -casein by electrostatic affinity chromatography. *Biochimica et Biophysica Acta (BBA) - Protein Structure*, 490, 255–259.
- Swaisgood, H. (2003). Chemistry of the caseins. In P. L. H. McSweeney, & P. F. Fox (Eds.), *Advanced dairy chemistry: Vol. 1. Proteins* (pp. 139–201). Boston, MA, USA: Springer.
- Visser, S., Slangen, C. J., & Rollema, H. S. (1991). Phenotyping of bovine milk proteins by reversed-phase high-performance liquid chromatography. *Journal of Chromatography A*, 548, 361–370.